Provided for non-commercial research and education use.
Not for reproduction, distribution or commercial use.

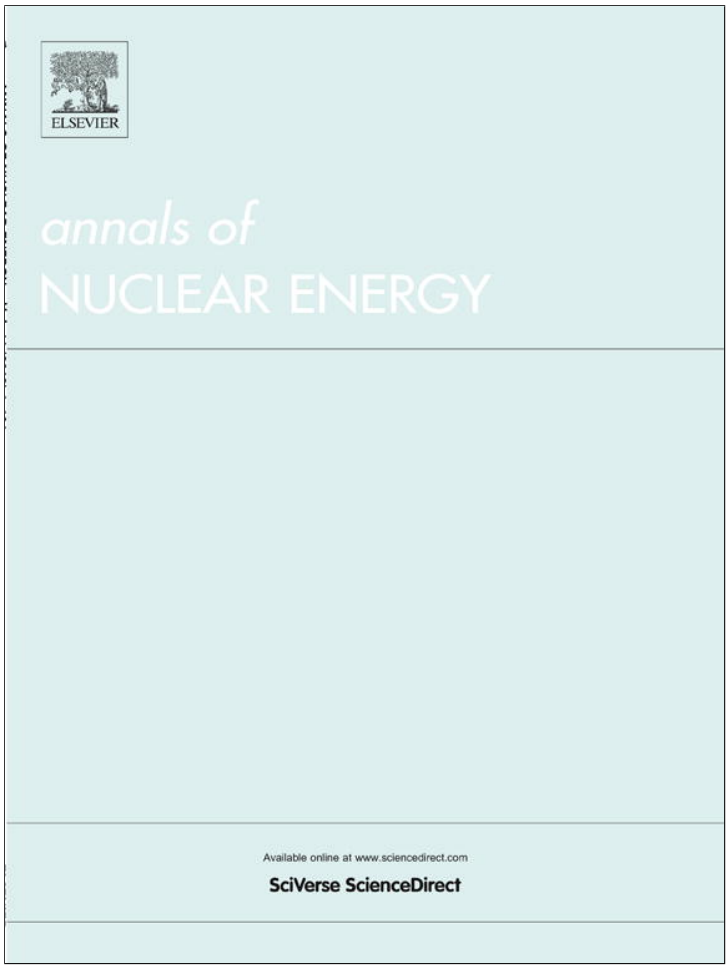

(This is a sample cover image for this issue. The actual cover is not yet available at this time.)

This article appeared in a journal published by Elsevier. The attached copy is furnished to the author for internal non-commercial research and education use, including for instruction at the authors institution and sharing with colleagues.

Other uses, including reproduction and distribution, or selling or licensing copies, or posting to personal, institutional or third party websites are prohibited.

In most cases authors are permitted to post their version of the article (e.g. in Word or Tex form) to their personal website or institutional repository. Authors requiring further information regarding Elsevier's archiving and manuscript policies are encouraged to visit:

http://www.elsevier.com/copyright

Author's personal copy

University of Utah Institutional Repository
Author Manuscript

Annals of Nuclear Energy 50 (2012) 220–231

Contents lists available at SciVerse ScienceDirect

Annals of Nuclear Energy

journal homepage: www.elsevier.com/locate/anucene

Validation of energy moments from the one-dimensional energy dependent neutron diffusion equation, MCNP5 and Attila-7.1.0 with the GODIVA experiment

Douglas S. Crawford [a,*], Terry A. Ring [b]

[a] Center for Space Nuclear Research/Idaho National Lab, 995 University Blvd., Idaho Falls, ID 83402, USA
[b] University of Utah, Chemical Engineering Department, 50 S. Central Campus Dr., Rm. 3290, Salt Lake City, UT 84112, USA

ARTICLE INFO

Article history:
Received 23 February 2012
Received in revised form 2 May 2012
Accepted 4 May 2012

Keywords:
Energy moments
Statistic's moments
GODIVA
Neutron
Diffusion
MCNP5

ABSTRACT

Normalized neutron energy moments (moments) from the one-dimensional energy dependent neutron diffusion equation (EDNDE), Monte Carlo N Particle 5 version 1.40 (MCNP5) and Attila-7.1.0-beta version (Attila) are validated with the GODIVA experiment (GODIVA). Energy moments 0–5 for all three methods are compared to GODIVA moments. GODIVA moments are measured with two methods. The 1st method is a time of flight (T-O-F) measurement of the average energy (moment 1) of the leaking neutrons from the surface of GODIVA and the 2nd method is from back calculating moments from foil activation analysis of various metal foils at the center of GODIVA. The error range of the EDNDE normalized moments compared to GODIVA is from 0% to 24%. The MCNP5 error range compared to GODIVA is 0–12% and the Attila error range is 0–79%. The method of moments is shown to be a fast reliable method, compared to either Monte Carlo methods (MCNP5) or 30 multi-energy group methods (Attila) with regard to the GODIVA experiment.

© 2012 Elsevier Ltd. All rights reserved.

1. Introduction

This work is focused on validating the method of moments for the EDNDE with GODIVA as well as further the development of the method by investigating the method of moments on a system of more than one isotope. Analytic energy moments derived for a pure 100% sphere of ^{235}U has been verified with MCNP5 and Attila based on the method of moment approach. The derivation for the method of moments for the EDNDE is not discussed here but can be found in literature (Crawford and Ring, accepted for publication). Eq. (1) is the basis of the normalized moments in this work (Duderstadt and Hamilton, 1976, p. 140).

$$\frac{1}{v}\frac{\partial\phi(\vec{r},E,t)}{\partial t} - \nabla D(\vec{r},E)\nabla\phi(\vec{r},E,t) + \Sigma_t(\vec{r},E)\phi(\vec{r},E,t) = \int_0^\infty \Sigma_s(\vec{r},E\rightarrow E')\phi(\vec{r},E',t)dE' + S(\vec{r},E,t) \quad (1)$$

The method of moments (MOM) approach solves for the moments of a distribution instead of the distribution itself. The mathematical definition of a raw moment is $m_k \equiv \int_0^\infty E^k\phi(\vec{r},E)dE$ where $k = 0, 1, 2, 3,\ldots, N$ (Casella and Berger, 2002); N is the total number of moments desired. MOM can be considered to be a deterministic method to find stochastic parameters. The neutron flux can be treated as a probability density function (PDF), where the normalized moments provide the mean, variance, skewness and kurtosis (Kenny, 1947) of the flux so once the moments are solved for they can be put into the correct PDF or PDF reconstruction method to reproduce the flux. Mathematically the mean, variance, skewness and kurtosis (Casella and Berger, 2002) for the energy variable of the neutron flux are represented here where ϕ in Eqs. (2)–(5) represent the energy dependent neutron flux $\phi(\vec{r},E,t)$:

$$\text{mean} = \frac{\int_0^\infty E * \phi dE}{\int_0^\infty \phi dE} \quad (2)$$

$$\text{variance} = \frac{\int_0^\infty E^2 * \phi dE}{\int_0^\infty \phi dE} \quad (3)$$

$$\text{skewness} = \frac{\int_0^\infty E^3 * \phi dE}{\int_0^\infty \phi dE} \quad (4)$$

$$\text{kurtosis} = \frac{\int_0^\infty E^4 * \phi dE}{\int_0^\infty \phi dE} \quad (5)$$

To help determine the proper PDF or PDF reconstruction method, neutron energy moments need to be validated.

This paper compares moments from MCNP5, Attila and 1-dimensional analytic moments from EDNDE (Eqs. (21)–(26)); with energy moments from the GODIVA experiment. GODIVA is a well documented experiment. Two documents were used as the foundation for the details of the computer/mathematical model

* Corresponding author. Tel.: +1 8015051409.
E-mail address: douglas.crawford@inl.gov (D.S. Crawford).

0306-4549/$ - see front matter © 2012 Elsevier Ltd. All rights reserved.
http://dx.doi.org/10.1016/j.anucene.2012.05.026

UU IR Author Manuscript
UU IR Author Manuscript

Author's personal copy

University of Utah Institutional Repository
Author Manuscript

creation of GODIVA in MCNP5, Attila and the EDNDE. The first document is from the International Handbook of Evaluated Criticality Safety Benchmark Experiments (INL NEA/NSC DOC(95)03, Septemberm 2010) and the second is a report outlining experiments done to measure ^{235}U fission spectrum at the core center and on the surface of GODIVA (McElroy et al., 1969). This report is referred to as the McElroy report for the rest of the paper. For a complete comparison of energy moments three computational platforms; MCNP5, Attila and EDNDE are compared to moments from the data in the McElroy report. MCNP5 and Attila are full neutron transport codes. MCNP5 is based on the Monte Carlo numerical method; Attila is a 30 energy group, S_N, P_N, finite element code. Table 1 shows the energy groups in the Attila 30 group library.

2. Simplification of EDNDE

Eq. (1) is solved over the entire fission spectrum; which is well approximated to be from 0 to 10 MeV (Lamarsh, 1966). This analysis assumes steady state so the time dependent term, $\frac{1}{v}\frac{\partial\phi(\vec{r},E)}{\partial t}$ is set equal to zero so Eq. (1) becomes Eq. (6).

$$-\nabla D(\vec{r},E)\nabla\phi(\vec{r},E)+\Sigma_t(\vec{r},E)\phi(\vec{r},E)=\int_0^\infty \Sigma_s(\vec{r},E\to \acute{E})\phi(\vec{r},\acute{E})d\acute{E}+S(\vec{r},E) \tag{6}$$

GODIVA is assumed to be homogenous so the energy dependent cross sections and diffusion coefficient depend on energy only Eq. (7) is the result.

$$-D(E)\nabla^2\phi(\vec{r},E)+\Sigma_t(E)\phi(\vec{r},E)=\int_0^\infty \Sigma_s(E\to \acute{E})\phi(\vec{r},\acute{E})d\acute{E}+S(\vec{r},E) \tag{7}$$

The integral $\int_0^\infty \Sigma_s(\vec{r},E\to\acute{E})\phi(\vec{r},\acute{E})d\acute{E}$ can be simplified by assuming $\phi(\vec{r},\acute{E})=\phi(\acute{E})\phi(\vec{r})$ and approximating $\phi(\acute{E})\cong\frac{1}{\acute{E}\Sigma_s(\acute{E})}$ and $\Sigma_s(\vec{r},E\to\acute{E})=\begin{cases}\frac{\Sigma_s(\acute{E})}{(1-\alpha)\acute{E}} & \text{for } E<\acute{E}<E/\alpha\\ 0 & \text{otherwise}\end{cases}$ where $\alpha\equiv\left(\frac{(A-1)}{(A+1)}\right)^2$ where A is the atomic weight of the isotope (Duderstadt and Hamilton, 1976, pp. 318–319). The approximations for the differential scattering cross section $(\Sigma_s(E\to\acute{E}))$ assumed in this research also assume two body collision kinematics and isotropic scattering in the center of mass system. Substituting the assumptions into the integral gives the following result in Eq. (8).

$$\int_E^{E/\alpha}\frac{\Sigma_s(\vec{E})}{(1-\alpha)\vec{E}}\frac{\phi(\vec{r})}{\vec{E}\Sigma_s(\vec{E})}d\vec{E}=\left(\frac{\phi(\vec{r})}{(1-\alpha)}\right)\left(\frac{(1-\alpha)}{E}\right)=\frac{\phi(\vec{r})}{E} \tag{8}$$

The range for E (0–10 MeV) assumed in this paper is large enough to capture the entire energy range of interest for most nuclear reactor calculations including the GODIVA critical assembly experiment. Only neutron downscattering is considered in this paper and upscattering is assumed very small. The result in Eq. (8) can be substitituted back into Eq. (7) and the result is Eq. (9).

$$-D(E)\nabla^2\phi(\vec{r},E)+\Sigma_t(E)\phi(\vec{r},E)=\frac{\phi(\vec{r})}{E}+S(\vec{r},E) \tag{9}$$

Eq. (9) is further simplified by multipling the numerator and demominator of $\frac{\phi(\vec{r})}{E}$ by $\Sigma_s(E)$ and make the assumption $\phi(\vec{r},E)=\phi(E)\phi(\vec{r})$ and approximating $\phi(E)\cong\frac{1}{E\Sigma_s(E)}$ this leads to Eq. (10). Then

$$-D(E)\nabla^2\phi(\vec{r},E)+\Sigma_t(E)\phi(\vec{r},E)=\frac{\phi(\vec{r})\Sigma_s(E)}{E\Sigma_s(E)}+S(\vec{r},E) \tag{10}$$

The right hand side of Eq. (10) is just $\Sigma_s(E)\phi(\vec{r},E)$. Eq. (10) can be simplified further by the following standard cross section convention shown in Eq. (11) (Duderstadt and Hamilton, 1976, p. 22) and Eq. (12) is the result.

$$\Sigma_t(E)=\Sigma_a(E)+\Sigma_s(E) \tag{11}$$

$$-D(E)\nabla^2\phi(\vec{r},E)+(\Sigma_a(E)+\Sigma_s(E))\phi(\vec{r},E)=\Sigma_s(E)\phi(\vec{r},E)+S(\vec{r},E) \tag{12}$$

Eq. (12) is simplified further by subtracting $\Sigma_s(E)\phi(\vec{r},E)$ from both sides of the equaiton and now the source term S is inserted as $\nu(E)\Sigma_f(E)\phi(\vec{r},E)$. The uniqueness to the method of moments approach to solving the EDNDE is that there is not a fission spectrum weighting on the source term. The energy range also spans nearly 100% of the fission spectrum. The fission spectrum integrated from 0 to 10 MeV is approximately unity $(\int_0^{10\text{MeV}}\chi(E)dE\cong 1)$. The neutron flux above that energy is very small and assumed to be negligible. The entire population of neutrons is treated as one large energy group E, from 0 to 10 MeV. The collection of assumption allows the energy dependence of the cross sections over the range of interest, 0–10 MeV to be retained and is contained within the energy moments as follows staring with Eq. (13).

$$-D(E)\nabla^2\phi(\vec{r},E)+\Sigma_a(E)\phi(\vec{r},E)=\nu(E)\Sigma_f(E)\phi(\vec{r},E) \tag{13}$$

A rearrangement of the cross sections in Eq. (13) give Eq. (14).

$$\nabla^2\phi(\vec{r},E)+\left(\frac{\nu(E)\Sigma_f(E)-\Sigma_a(E)}{D(E)}\right)\phi(\vec{r},E)=0 \tag{14}$$

We have assumed diffusion theory is applicable and consider only the 1-D analytic solution, for the EDNDE moments based on the shape (sphere) and isotopic concentrations of the GODIVA experiment. Neutron diffusion theory is well documented in literature (Duderstadt and Hamilton, 1976; Foster and Wright, 1977; Lamarsh and Baratta, 2001; Lewis and Miller, 1993; Weinberg and Wigner, 1958) and is not discussed in detail here. An average angle of scatter for the neutrons $\bar{\mu}_o$ is also assumed and included in the neutron diffusion coefficient (Lamarsh, 1966, p. 56). Derivation of $\bar{\mu}_o$ is not included and can be found in literature (Duderstadt and Hamilton, 1976; Foster and Wright, 1977; Lamarsh and Baratta, 2001; Lewis

Table 1
Energy group structure for GODIVA model in Attila-7.1.0-beta.

Group #	Energy range (MeV)		Group #	Energy range (MeV)		Group #	Energy range (MeV)	
1	2.00E+01	1.70E+01	11	7.79E+00	6.87E+00	21	8.21E−01	2.35E−01
2	1.70E+01	1.60E+01	12	6.87E+00	6.07E+00	22	2.35E−01	6.74E−02
3	1.60E+01	1.50E+01	13	6.07E+00	5.35E+00	23	6.74E−02	1.93E−02
4	1.50E+01	1.39E+01	14	5.35E+00	4.72E+00	24	1.93E−02	5.53E−03
5	1.39E+01	1.30E+01	15	4.72E+00	3.68E+00	25	5.53E−03	3.54E−04
6	1.30E+01	1.20E+01	16	3.68E+00	2.87E+00	26	3.54E−04	2.26E−05
7	1.20E+01	1.10E+01	17	2.87E+00	2.23E+00	27	2.26E−05	3.47E−06
8	1.10E+01	1.00E+01	18	2.23E+00	1.74E+00	28	3.47E−06	6.25E−07
9	1.00E+01	8.82E+00	19	1.74E+00	1.19E+00	29	6.25E−07	1.24E−08
10	8.82E+00	7.79E+00	20	1.19E+00	8.21E−01	30	1.24E−08	1.00E−11

UU IR Author Manuscript
UU IR Author Manuscript

Author's personal copy

University of Utah Institutional Repository
Author Manuscript

UU IR Author Manuscript

and Miller, 1993; Weinberg and Wigner, 1958). The equations to describe $D(E)$ and $\bar{\mu}_o$ are Eq. (19) and Eq. (21) respectively. Lumping all of the energy dependent cross sections and parameters into one function of energy $F(E)$ Eq. (15) leads to Eq. (16), where B^2_{Ek} is similar to a buckling term for each raw neutron energy moment and subject to the standard diffusion boundary conditions, flux is finite everywhere and at the extrapolated boundary flux is 0. Eq. (17) shows the extrapolated neutron boundary condition in raw moment form.

$$F(E) = \frac{\nu(E)\Sigma_f(E) - \Sigma_a(E)}{D(E)} = 3(\nu(E)\Sigma(E)_f - \Sigma_a(E))(\Sigma_t(E) - \bar{\mu}\Sigma_s(E)) \quad (15)$$

$$\int_0^\infty E^k \nabla^2 \phi(\vec{r},E)dE + \int_0^\infty E^k F(E)\phi(\vec{r},E)dE + \int_0^\infty E^k B^2_{Ek}\phi(\vec{r},E)dE = 0 \quad (16)$$

$$m_k(\widetilde{R}) = \int_0^\infty E^k \phi(r = \widetilde{R}_k, E)dE = 0 \quad (17)$$

The solution to the extrapolated boundary condition lead to the moment buckling terms to be the following $B_{E0} = \frac{\pi}{R_0}$ and $B_{Ek} = \frac{3\pi}{4R_k}$ for $k = 1, 2, 3, \ldots, N$. The derivation for the diffusion boundary conditions is not shown here and can be seen in literature (Crawford and Ring, accepted for publication).

The equation solved for is the moment form of the EDNDE which is Eq. (18).

$$\nabla^2 m_k + B^2_{Ek} \cdot m_k + \int_0^\infty E^k F(E)\phi(\vec{r},E)dE = 0 \quad (18)$$

The derivation of the analytic moments from the EDNDE for GODIVA is shown in the next section. An overall energy dependent function $F(E)$ is also derived for the isotopic mix of GODIVA.

3. Derivation of F(E) and neutron energy moments for GODIVA

An appropriate approximation to the energy dependency of the macroscopic cross sections and the diffusion coefficient is vital for any flux calculation; so a set of functions and constants have been carefully chosen so the energy dependent functionality is retained as much as possible and allow an analytic solution to be found. The macroscopic cross sections may generally be divided into three distinct regions: thermal, resonance and fast, and in this paper the authors consider a 4th region called the transition region and it spans from 2300 eV to 1 MeV. The reason for the subdivisions is explained in more detail below.

The $1/v$ or $1/E^{1/2}$ law is a good approximation to the thermal region of many isotopes and found to be mathematically viable in foil activation (Morry and Williams, 1972). The cross section data referred to and in use for this paper is from the evaluated nuclear data files, ENDF information is found on the web at http://atom.kaeri.re.kr/ (Institute, 2000) and http://t2.lanl.gov/data/neutron7.html) (Lab, ENDF/B-VII Incident-Neutron Data, 2000). In the resonance region, a summation of functions similar to Breit–Wigner single level resonance formulas is used to capture the complicated energy dependence in the resonance region. The functional piece that dominates the Breit–Wigner formulas is this $\left(\frac{\text{Constant}_1}{(E-E_r)^2+\text{Constant}_2}\right)$ term (Lamarsh, 1966, pp. 43–64). The cross sections for many isotopes in the transition region to the fast region generally has a $1/E$ drop off rate (Weinberg and Wigner, 1958, p. 57) and the fast region (0.1–10 MeV) has a $1/E^{5/2}$ with some broad resonances. The broad resonances give the fast region of ^{235}U $\Sigma_f(E)$ somewhat of a stair step like shape from 1 MeV to 20 MeV.

It is very difficult to fit an analytic function to the resonance region and the broad resonance region. The number of resonance peaks makes writing a function for each peak a daunting task, but with patience a resonance function can be written for each peak. A resonance peak function has been written for 962 resonances in this work for the GODIVA $F(E)$, see (Tables A1–A3) in Appendix A. A summation of these single level resonance functions was assembled to provide a functional form, that when integrated over the function would provide correct values when compared to the resonance values from *The Chart of the Nuclides and Isotopes 16th Edition* (Lockheed Martin/ Knolls Atomic Power Laboratory, 2002). The functional approximations for the energy dependent cross sections are somewhat crude but "if we choose the group constants properly, even one-speed diffusion theory could give an accurate description of nuclear reactor behavior" (Duderstadt and Hamilton, 1976, p. 295).

The general functional relationships for $D(E)$, $\nu(E)$, $\Sigma_f(E)$, $\Sigma_T(E)$, $\Sigma_S(E)$ and $\Sigma_a(E)$ with energy are incorporated into one function of energy $F(E)$. This work only shows curve fits of $F(E)$ for the isotopic mix in GODIVA. The derived $F(E)$ is fit to ENDF–$F(E)$ with the appropriate function fit for the different energy ranges. The result of the curve fit of $F(E)$ is shown in Eq. (20) and Figs. 1–5.

It is assumed the total macroscopic cross section, the transport cross section, the function $\nu(E)$ (the number of prompt neutrons released in fission by an incident neutron of energy E), the neutron diffusion coefficient and the average angle of scatter are:

$$\Sigma(E)_{tr} = \Sigma(E)_t - \bar{\mu}_o\Sigma(E)_s \quad (19)$$

$$D(E) = \frac{1}{3\Sigma_{tr}(E)} = \frac{1}{3(\Sigma_{tr}(E) - \bar{\mu}_i\Sigma_s(E))} \quad (20)$$

$$\nu(E) = \nu_s E + \upsilon_{s0} \quad \text{for } 0 \leqslant E \leqslant 1 \text{ MeV} \quad (21)$$

$$\nu(E) = \nu_f E + \upsilon_{f0} \quad \text{for } E > 1 \text{ MeV} \quad (22)$$

$$\bar{\mu}_0 = \frac{2}{3A} \quad (23)$$

$$\bar{\mu}_{0,\text{system}} = \sum_i^N \omega_i \bar{\mu}_{o,i} \quad (24)$$

ω_i = atom fraction of istope i, N is total number of isotpes.

In Eq. (24), the capital Greek letter sigma is a summation term not a cross section. The parameter, A_i in Eq. (24) is the atomic mass number of isotope (i), N in Eq. (24) is the total number of isotopes in the reactor, i.e. for GODIVA $N = 3$. The convention for a mix of isotopes is Eq. (25).

$$\Sigma_j^{\text{system}} = \Sigma_j^{^{235}_{92}\text{U}} + \Sigma_j^{^{238}_{92}\text{U}} + \Sigma_j^{^{234}_{92}\text{U}} \quad (25)$$

Index j in Eq. (25) is the subscript to represent the specific nuclear reaction: fission (f), scatter (s), absorption (a), etc. This convention is used to calculate the system cross sections for GODIVA and is the standard convention in most nuclear textbooks. Eq. (23) is a decent

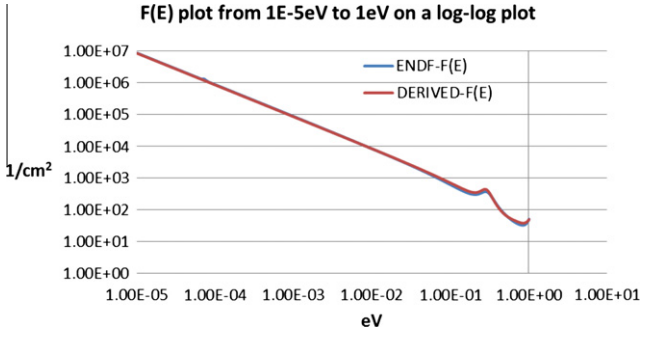

Fig. 1. Log–log plot of GODIVA F(E) from 1E−5 eV to 1 eV.

Author's personal copy

University of Utah Institutional Repository
Author Manuscript

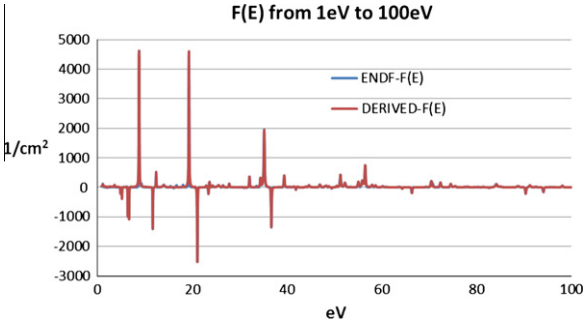

Fig. 2. Plot of GODIVA $F(E)$ from 1 eV to 100 eV.

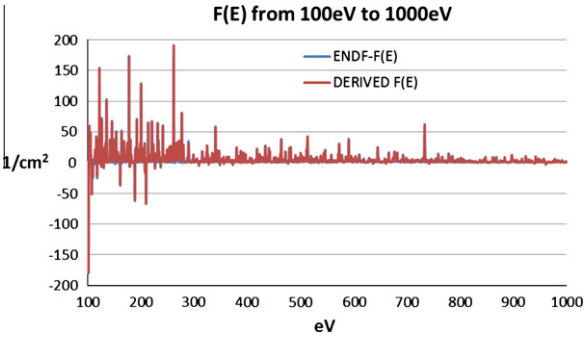

Fig. 3. Plot of GODIVA $F(E)$ comparison from 100 eV to 1000 eV.

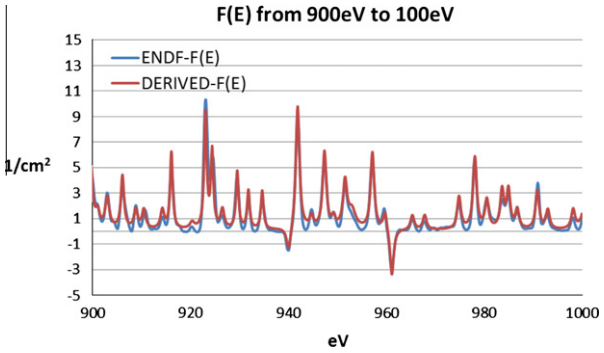

Fig. 4. Close view of GODIVA $F(E)$ and the overlap between resonance peaks.

approximation for the average angel of scatter, $\bar{\mu}_o$ for large atoms i.e. $A > 16$. The function $\nu(E)$ is approximated for the isotopic mix of GODIVA where the $\nu(E)$ parameters for ^{235}U is $\nu = 0.066$, $\upsilon_{s0} = 2.432$, $\nu_f = 0.15$ and $\upsilon_{f0} = 2.349$ (Duderstadt and Hamilton, 1976, p. 61) if the energy variable is in units of MeV. The parameters of $\nu(E)$ for ^{238}U are $\nu_s = 0.16$, $\upsilon_{s0} = 2.3$ for all energies (Lamarsh, 1966, p. 96 Tables 3–5) and for ^{234}U $\nu_s = 0.117$, $\upsilon_{s0} = 2.45$ for all energies. The slope and intercept of $\nu(E)$ for ^{234}U are derived from the data provided by Los Alamos National Lab (Lab, ENDF/B-VII Incident-Neutron Data, 2000); the energy variable is in units of MeV. The parameters of $\nu(E)$ for the isotope mix of GODIVA are $\nu_s = 0.071$, $\upsilon_{s0} = 0.425$, $\nu_f = 0.15$ and $\upsilon_{f0} = 2.347$. Figs. 1–5 show comparisons of Eq. (26) with the ENDF–$F(E)$.

Fig. 1 shows the thermal region from 1E−5 eV to 1 eV on a log–log plot. The first term in Eq. (20) is the dominate feature in Fig. 1. The first resonance the GODIVA $F(E)$ is seen in Fig. 1. Figs. 2–5 are not put on log–log plots to point out the negative regions that show up from the $\nu(E)\Sigma_f(E) - \Sigma_a(E)$ term in $F(E)$, where the absorption cross section is greater than the product of $\nu(E)\Sigma_f(E)$.

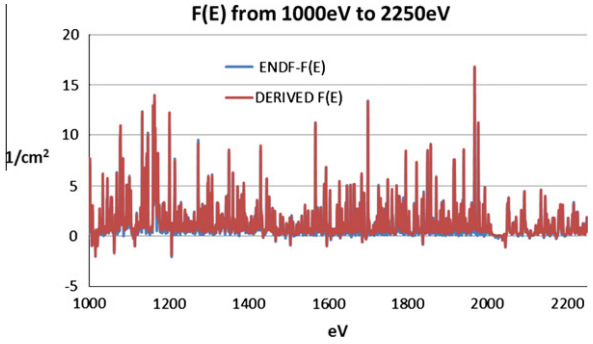

Fig. 5. Comparison plot of the derived GODIVA $F(E)$ to the ENDF GODIVA $F(E)$ in the energy range of 1000–2250 eV, the end of the resonance region.

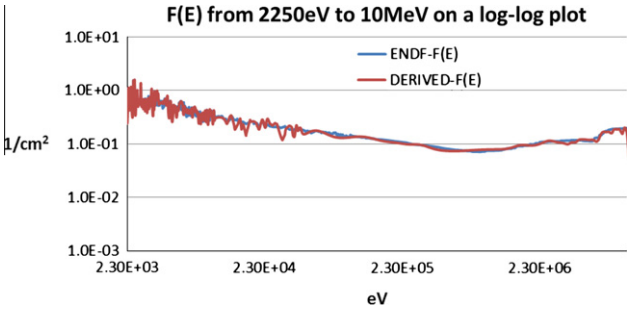

Fig. 6. Comparison of the two GODIVA $F(E)$ functions from 2250 eV to 10 MeV.

Fig. 2 shows a comparison of ENDF–$F(E)$ to Eq. (21) for GODIVA in the energy range of 1–100 eV to show the largest resonance peaks. Eq. (21) is not as sharp as the ENDF–$F(E)$ in the overlap spaces between each resonance peak.

Some of the minor peaks throughout the resonance region were not included into Eq. (21). The reason for doing this is because these small resonance peaks did not add enough value to the resonance integral value. Another reason for not including some small peaks into Eq. (21) is because Eq. (21) over estimates the overlap from resonance peak to resonance peak so the two effects seem to balance each other. The resonance values from *The Chart of the Nuclides and Isotopes 16th Edition* matched the resonance values from Eq. (21).

Fig. 5 shows the end of the resonance region and the beginning of the transition region.

Fig. 6 shows the transition region and the fast region up to 10 MeV.

$$F(E) = \frac{Rp_0}{E} + \sum_{l=1}^{N} \frac{Rp_l}{(E - Er_l)^2 + w_l} + \sum_{m=1}^{N_{TRANS}} \frac{Rp_m \cdot (\nu_s E + \upsilon_{s0})_{2300eVto1MeV}}{(E - Er_m)^2 + w_m} + \sum_{n=1}^{N_{FAST}} \frac{Rp_n \cdot (\nu_f E + \upsilon_{f0})_{E>1MeV}}{(E - Er_n)^4 + w_n \cdot E} \quad (26)$$

The constants from Eq. (26) are: $Rp_0[=]\frac{Energy}{cm^2}$, $Rp'_{l,m}s[=]\frac{Energy^2}{cm^2}$, $Er'_{l,m,n}s[=]Energy$, $w'_{l,m}s[=]Energy^2$, $Rp'_ns[=]\frac{Energy^4}{cm^2}$, $w'_ns[=]Energy^3$, $\nu_s\&$; $\nu_f[=]\frac{neutrons}{Energy}$ and $\upsilon_{s0}/\upsilon_{f0}[=]neutrons$, where N, N_{TRANS} and N_{FAST} are the number of terms included in each sum with indices l, m and n. The $Rp'_{l,m}s$ can be positive or negative because in some energy ranges $(-\Sigma(E)_a)$ is greater than $(\nu(E)\Sigma(E)_f)$. The data for each constant is in Appendix A. 832 individual terms,

UU IR Author Manuscript
UU IR Author Manuscript

Author's personal copy

University of Utah Institutional Repository
Author Manuscript

Table 2
List of the energy constants from $F(E)$ method of moment analysis for GODIVA.

Constant	Value	Units
CE1	0.052	MeV/cm^2
CE2	0.079	MeV^2/cm^2
CE3	0.310	MeV^3/cm^2
CE4	1.720	MeV^4/cm^2
CE5	12.185	MeV^5/cm^2

Table 3
The extrapolated boundaries for moment 0–5.

$\tilde{R}_0$	$\tilde{R}_1$	$\tilde{R}_2$	$\tilde{R}_3$	$\tilde{R}_4$	$\tilde{R}_5$
11.02 cm	11.08 cm	11.18 cm	11.19 cm	11.19 cm	11.19 cm

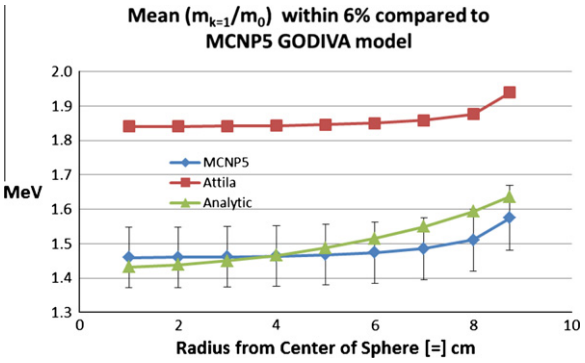

Fig. 7. Comparison plot of the mean energy for the GODIVA benchmark.

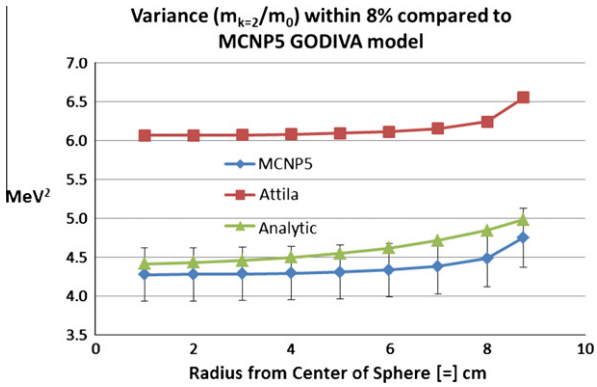

Fig. 8. Comparison plot of the variance of energy for the GODIVA benchmark.

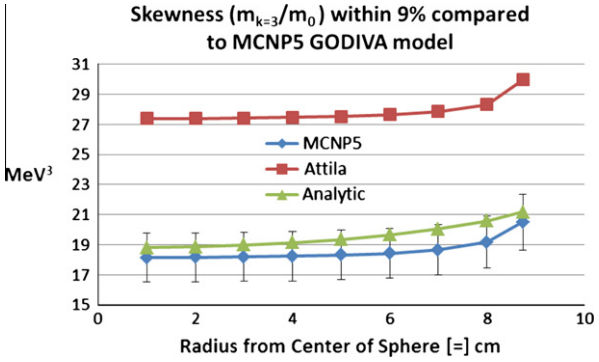

Fig. 9. Comparison plot of the skewness of energy for the GODIVA benchmark.

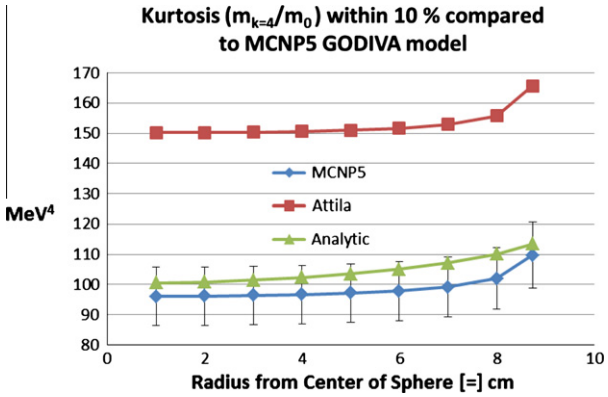

Fig. 10. Comparison plot of the kurtosis of energy for the GODIVA benchmark.

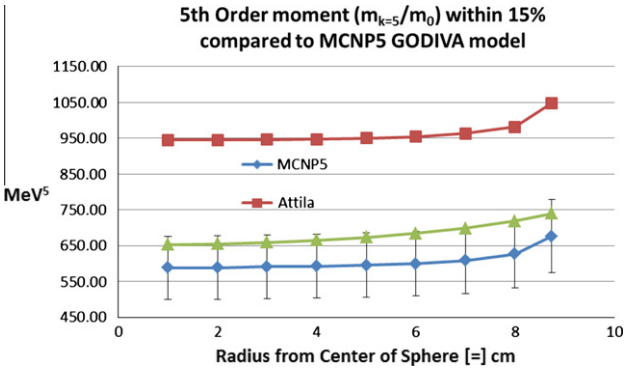

Fig. 11. Comparison plot of the 5th energy moment for the GODIVA benchmark.

$\left(\frac{Rp_l}{(E-Er_l)^2+w_l}\right)$ are accounted for in the first summation, 120 terms $\left(\frac{Rp_m\cdot(v_sE+v_{s0})_{2300eVto1MeV}}{(E-Er_m)^2+w_m}\right)$ in the second summation and 10 individual terms $\left(\frac{Rp_n\cdot(v_fE+v_{f0})_{E>1MeV}}{(E-Er_n)^4+w_n\cdot E}\right)$ are accounted for in the third summation of Eq. (26).

The first term $\frac{Rp_0}{E}$ and the first summation term $\sum_{l=1}^{N}\frac{Rp_l}{(E-Er_l)^2+w_l}$ in Eq. (20) were observable by visual inspection of the ENDF–$F(E)$ plot. The first term comes from the $1/v$ portions of the cross sections multiplied together. The first summation term captured ENFD–$F(E)$ in the energy range of 1–2250 eV. This range remained visually similar to the resonance region of ^{235}U $\Sigma(E)_t$ except for the few negative regions and the height/width of the each resonance peak which is specific to the GODIVA ENDF–$F(E)$ resonance peaks. The height and width of each ENDF–$F(E)$ peak can be matched by Eq. (26) by adjusting Rp_l and w_l respectively.

The second and third summation terms in Eq. (26) account for the linear effect of $v(E)$ on $F(E)$. The first and second terms of Eq. (26) are not affected by $v(E)$ because the slope is so small, just the constant affects $F(E)$ and it is absorbed into Rp_0 and the Rp_ls. The slope of $v(E)$ does not change the value of $v(E)$ until roughly 46 keV and only from 2.43 to 2.44. It is included in the energy range at 2300 eV because of the shape of ENDF–$F(E)$ from 2300 eV to 0.9 MeV is a rough $1/E$ function, which $\frac{Rp_m\cdot(v_sE+v_{s0})_{2300eVto1MeV}}{(E-Er_m)^2+w_m}$ is approximately a $1/E$ function. A summation of these terms $\frac{Rp_m\cdot(v_sE+v_{s0})_{2300eVto1MeV}}{(E-Er_m)^2+w_m}$ provided a few useful qualities to fit the ENDF–$F(E)$ from 2300 eV to 0.9 MeV. The first is an ability

UU IR Author Manuscript
UU IR Author Manuscript

Author's personal copy

University of Utah Institutional Repository
Author Manuscript

Table 4
Results of the GODIVA moments at the center of the sphere based on the foil activation measurements in the McElroy report.

Energy moments from GODIVA Core Center with Experiment Error from McElroy report					
m_0 unit less	m_1 [=] MeV	m_2 [=] MeV^2	m_3 [=] MeV^3	m_4 [=] MeV^4	m_5 [=] MeV^5
1 ± 5.6%	1.471 ± 5.6%	4.151 ± 5.6%	16.82 ± 5.6%	86.39 ± 5.6%	526.64 ± 5.6%
Energy moments from MCNP GODIVA at R = 1 cm with % relative error from GODIVA value					
m_0 unit less	m_1 [=] MeV	m_2 [=] MeV^2	m_3 [=] MeV^3	m_4 [=] MeV^4	m_5 [=] MeV^5
1 ± 0%	1.460 ± 0.7%	4.275 ± 3.0%	18.14 ± 7.8%	96.04 ± 11.2%	588.37 ± 11.7%
Energy moments from Analytic EDNDE GODIVA at R = 1 cm % relative Error from GODIVA value					
m_0 unit less	m_1 [=] MeV	m_2 [=] MeV^2	m_3 [=] MeV^3	m_4 [=] MeV^4	m_5 [=] MeV^5
1 ± 0%	1.430 ± 2.8%	4.41 ± 6.2%	18.79 ± 10.5%	100.38 ± 16.2%	652.48 ± 23.9%
Energy moments from Attila GODIVA at R = 1 cm %relative error from GODIVA value					
m_0 unit less	m_1 [=] MeV	m_2 [=] MeV^2	m_3 [=] MeV^3	m_4 [=] MeV^4	m_5 [=] MeV^5
1 ± 0%	1.84 ± 25.0%	6.069 ± 46.2%	27.40 ± 62.9%	150.16 ± 73.8%	944.87 ± 79.4%

Table 5
T-O-F measurement of the average energy (m_1) of the surface for GODIVA.

GODIVA m_1 T-O-F measurement at sphere surface	
m_1 [=] MeV	1.55 ± 2.9%*
MCNP m_1 at sphere surface	
m_1 [=] MeV	1.58 ± 2.0%**
Analytic EDNDE moment at sphere surface	
m_1 [=] MeV	1.64 ± 5.8%**
Attila moment at sphere surface	
m_1 [=] MeV	1.94 ± 25%**

to shift a $1/E$ function to this energy range at various places without the sharp discontinuity from these two $\frac{1}{(E-Er_m)}$ or $\frac{(v_s E+v_{s0})}{(E-Er_m)}$ functions or any similar function with an odd order in the denominator i.e. a term $\frac{1}{(E-Er_m)^{2n+1}}$ where $n = 0\ldots\infty$. The second reason this function is chosen is because it produced a smooth curve (see Fig. 6 from 0.1 MeV to 0.9 MeV) with a long forward tail which is the $1/E$ shape desired in this region without the sharp discontinuity. The third reason for this function is, small resonance peaks are in this energy range. The small peaks could be modeled with this function because it can be easily tuned by adjusting Rp_m and w_m to have a peak at the resonance energy Er_m.

The energy range 0.9–10 MeV yielded a different shape. In this energy range ENDF-$F(E)$ increased in a stair step shape (broad resonance) similar to the ^{235}U fission cross section shape from 0.9 to 10 MeV. The slope of $\nu(E)$ in this energy range is larger and the effect from this linear function is greater. The term inside the third summation, $\frac{Rp_n\cdot(\nu_f E+\nu_{f0})_{E>1\text{MeV}}}{(E-Er_n)^4+w_n\cdot E}$ is used for similar reasons already mentioned: a smooth curve without sharp discontinuities (no odd ordered denominators), an ability to add an increase or "peak" at a specific energy(Er_n). The denominator $((E-Er_n)^4+w_n\cdot E)$ allowed for a much broader peak and a sharper drop off creating the level stair effect that corresponds to the broad width of the peak. The $w_n\cdot E$ in the denominator along with the 4th order term$(E-Er_n)^4$ restricted any long forward or backward tail that is seen with this these denominator choices $((E-Er_n)^2+E\cdot w_n)$ and $((E-Er_m)^2+-w_n)$. The elimination of the long tails in this energy region was necessary to get the correct overlap between resonances; the other function choices investigated could not provide this effect in this energy region and consequently did not match the ENDF–$F(E)$.

These functions included into Eq. (20) allowed for analytic analysis and the development of analytic moments to be created.

4. Analytic neutron moments for GODIVA

The set of analytical energy dependent neutron moments are found from transforming the EDNDE with the definition of a raw moment subject to the neutron diffusion boundary conditions. The full derivation of Eq. (18) into the set of analytic energy dependent neutron moments is not discussed here and can be found in literature (Crawford and Ring, accepted for publication) along with the derivation to obtain the constants that come from the method of moment's analysis. Table 2 is a list of the constants found with Eq. (26) and the moment transformation needed for validation of normalized neutron energy moments with the GODIVA experiment.

The set of moments that are plotted for comparison are the normalized moments. The moments $m_k = 1, 2, 3, 4, 5$ are normalized by the 0th moment, m_0. The normalized moments provide information about the population density function i.e. mean energy (m_1/m_0), variance of the energy (m_2/m_0), skewness (m_3/m_0) and kurtosis (m_4/m_0). The normalized energy dependent neutron diffusion moments (NEDNDM) are seen in Eqs. (27)–(32), where $a_0 = 1$. The set of normalized moments, m_k/m_0:

$$\frac{m_0}{m_0}=\frac{a_0\frac{\sin(B_{E0}\cdot r)}{r}}{a_0\frac{\sin(B_{E0}\cdot r)}{r}}\equiv 1 \tag{27}$$

$$\frac{m_1}{m_0}=\frac{a_1\sin(B_{E1}\cdot r)}{a_0\sin(B_{E0}\cdot r)}+\frac{b_1 r\cos(B_{E1}\cdot r)}{a_0\sin(B_{E0}\cdot r)} \tag{28}$$

$$\frac{m_2}{m_0}=\frac{a_2\sin(B_{E2}\cdot r)}{a_0\sin(B_{E0}\cdot r)}+\frac{b_2 r\cos(B_{E2}\cdot r)}{a_0\sin(B_{E0}\cdot r)}+\frac{c_2 r^2\sin(B_{E2}\cdot r)}{a_0\sin(B_{E0}\cdot r)} \tag{29}$$

$$\frac{m_3}{m_0}=\frac{a_3\sin(B_{E3}\cdot r)}{a_0\sin(B_{E0}\cdot r)}+\frac{b_3 r\cos(B_{E3}\cdot r)}{a_0\sin(B_{E0}\cdot r)}+\frac{c_3 r^2\sin(B_{E3}\cdot r)}{a_0\sin(B_{E0}\cdot r)}+\frac{d_3 r^3\cos(B_{E3}\cdot r)}{a_0\sin(B_{E0}\cdot r)} \tag{30}$$

$$\frac{m_4}{m_0}=\frac{a_4\sin(B_{E4}\cdot r)}{a_0\sin(B_{E0}\cdot r)}+\frac{b_4 r\cos(B_{E4}\cdot r)}{a_0\sin(B_{E0}\cdot r)}+\frac{c_4 r^2\sin(B_{E4}\cdot r)}{a_0\sin(B_{E0}\cdot r)}+\frac{d_4 r^3\cos(B_{E4}\cdot r)}{a_0\sin(B_{E0}\cdot r)}+\frac{e_4 r^4\sin(B_{E4}\cdot r)}{a_0\sin(B_{E0}\cdot r)} \tag{31}$$

$$\frac{m_5}{m_0}=\frac{a_5\sin(B_{E5}\cdot r)}{a_0\sin(B_{E0}\cdot r)}+\frac{b_5 r\cos(B_{E5}\cdot r)}{a_0\sin(B_{E0}\cdot r)}+\frac{c_5 r^2\sin(B_{E5}\cdot r)}{a_0\sin(B_{E0}\cdot r)}+\frac{d_5 r^3\cos(B_{E5}\cdot r)}{a_0\sin(B_{E0}\cdot r)}+\frac{e_5 r^4\sin(B_{E5}\cdot r)}{a_0\sin(B_{E0}\cdot r)}+\frac{f_5 r^5\cos(B_{E5}\cdot r)}{a_0\sin(B_{E0}\cdot r)} \tag{32}$$

The extrapolated boundaries for GODIVA are in Table 3. All of the other constants (a_1 to a_5, b_1 to b_5, c_2 to c_5, d_3 to d_5, e_4 to e_5 and f_5) are derived from the constants reported in Tables 2 and 3.

The normalized moments from MCNP, Attila and NEDNDM are plotted in Figs. 6–10 in Section 5 of the paper. There are three

UU IR Author Manuscript
UU IR Author Manuscript

Author's personal copy

University of Utah Institutional Repository
Author Manuscript

Table A1
List of the $Rp_i's, Er_i's$ and $w_i's$.

$Rp_i's$	$Er_i's$	$w_i's$	$Rp_i's$	$Er_i's$	$w_i's$	$Rp_i's$	$Er_i's$	$w_i's$
−37.5	0.18	0.19	0.9	506.01	0.2	0.3	1254.05	0.25
0.99	0.28	0.0035	0.6	507.89	0.087	0.3	1255.81	0.3
−1.05	0.85	0.065	0.6	510.03	0.087	0.3	1258.17	0.25
0.24	1.12	0.003	1.8	511.48	0.087	1.5	1263.12	0.7
−0.6	2.04	0.015	3.6	513.21	0.087	0.3	1267.02	0.4
0.12	3.6	0.002	0.75	519.66	0.087	0.3	1268.31	0.5
−0.3	4.85	0.0013	0.45	520.6	0.1	0.45	1270	0.5
−0.36	5.16	0.0009	0.54	524.36	0.1	2.25	1273	0.25
1.05	6.3	0.015	0.54	527.85	0.087	0.6	1278.46	0.25
−1.14	6.39	0.0011	2.4	530.33	0.3	0.45	1280.37	0.25
0.3	6.54	0.004	0.24	535.37	0.087	0.75	1283.72	0.25
−1.23	6.68	0.0011	0.3	536.91	0.087	0.15	1287.5	0.5
0.54	6.81	0.012	0.9	537.91	0.087	0.66	1290.61	0.25
12	8.78	0.0026	0.3	539.91	0.2	0.3	1291.89	0.3
−1.2	11.67	0.0009	0.45	542.15	0.087	1.2	1296.89	0.25
0.96	12.38	0.0019	1.5	543.78	0.1	1.35	1298.63	0.25
2.7	13.96	0.04	1.95	546.22	0.1	0.3	1300.78	0.25
13.8	19.3	0.003	0.3	551.8	0.1	0.9	1305.59	0.225
−6	21.07	0.0024	0.45	556.41	0.1	0.9	1308	0.16
0.39	22.94	0.0064	1.2	557.77	0.1	0.15	1311.8	0.25
−0.99	23.41	0.004	0.3	561	0.1	0.06	1315.05	0.25
0.18	20.61	0.005	0.3	564.75	0.1	0.21	1317.07	0.25
0.99	21.32	0.014	0.3	566.74	0.1	0.15	1318.9	0.25
0.99	23.63	0.005	0.6	570.98	0.05	0.75	1320.87	0.25
0.27	24.29	0.0045	3.3	572.51	0.11	0.75	1323.3	0.25
3.3	25.55	0.0475	1.8	575.83	0.2	0.3	1326.05	0.25
0.27	26.5	0.0045	2.19	577.64	0.2	0.45	1329.83	0.25
0.54	27.79	0.0045	0.24	579.51	0.1	0.45	1332.23	0.25
1.26	32.07	0.0035	0.75	585.22	0.1	0.45	1333.8	0.25
−0.06	31.44	0.0035	0.57	585.83	0.1	0.15	1335.5	0.25
−0.06	30.9	0.0035	0.6	587.54	0.1	0.36	1336.99	0.25
2.25	34.38	0.0075	3.6	590.63	0.1	0.3	1338.75	0.25
15	35.18	0.0078	0.6	592.03	0.1	0.9	1343.01	0.25
−4.05	36.68	0.003	0.24	593.47	0.1	2.7	1346.56	0.75
3	39.4	0.0075	0.9	595.02	0.1	0.84	1350.41	0.1
0.15	40.52	0.0095	0.6	595.97	0.1	0.3	1355.6	0.25
1.2	41.51	0.0475	0.51	598.94	0.1	0.3	1358.8	0.25
−0.24	41.86	0.0025	0.42	600.4	0.1	1.5	1360.37	0.25
0.24	42.24	0.0125	2.25	603.22	0.25	0.24	1363.28	0.25
−0.09	42.68	0.01	1.05	604.4	0.25	0.3	1364.07	0.25
−0.09	43.36	0.01	0.54	608.46	0.25	0.3	1367.66	0.25
0.24	43.96	0.01	1.8	610.21	0.15	1.2	1372.05	0.25
1.05	44.61	0.015	0.6	612.9	0.25	0.6	1378.2	0.18
1.35	46.93	0.015	0.6	615.43	0.25	0.45	1380.7	0.3
0.45	47.98	0.015	0.6	616.89	0.25	0.69	1382.1	0.18
0.75	48.3	0.015	1.05	619.02	0.25	2.55	1387.6	0.5
0.24	48.8	0.008	0.6	626.6	0.25	0.45	1390.26	0.25
−0.24	49.43	0.0063	1.05	628.99	0.2	0.6	1393.8	0.4
0.3	50.48	0.0063	0.45	630.8	0.25	0.6	1395.3	0.45
3.45	51.26	0.0083	0.45	631.69	0.25	0.15	1397.37	0.25
3	52.21	0.02	1.05	633.64	0.275	0.15	1400.75	0.25
1.8	55.04	0.01	1.05	635.41	0.25	0.3	1403.45	0.25
5.25	55.88	0.025	−0.6	636.5	0.25	0.45	1406.4	0.25
6.6	56.48	0.009	1.05	639.14	0.25	0.36	1410.5	0.25
1.5	57.95	0.02	0.6	641.17	0.2	0.45	1415.29	0.25
1.2	58.66	0.02	2.4	644.96	0.1	0.63	1418.47	0.25
0.66	60.18	0.02	0.6	646.65	0.1	0.84	1421.17	0.25
0.3	60.84	0.03	0.3	648.83	0.2	0.3	1423.63	0.25
0.84	63.66	0.075	0.3	653.07	0.2	0.3	1425.77	0.25
−0.36	64.3	0.007	0.6	656.4	0.3	0.3	1427.2	0.25
−0.96	66.35	0.005	0.6	658.38	0.1	1.5	1430.07	0.175
0.3	69.29	0.03	−0.3	660.55	0.15	0.6	1431.75	0.35
3.75	70.46	0.018	0.6	663.6	0.15	0.6	1433.53	0.35
2.79	72.36	0.018	1.5	665.92	0.1	−0.15	1436.27	0.35
2.1	74.54	0.018	0.6	672.13	0.2	0.15	1439.5	0.35
1.2	75.49	0.03	1.35	674.11	0.2	0.15	1442.53	0.35
0.3	77.5	0.03	3	676.42	0.2	1.5	1445.29	0.27
0.6	78.11	0.03	7.2	678.07	0.7	0.75	1449.75	0.25
0.3	79.68	0.04	2.25	681.79	0.15	0.9	1451.81	0.25
0.42	80.34	0.04	0.6	683.82	0.5	0.24	1454.09	0.25
0.3	81.42	0.02	0.6	685.53	0.5	0.24	1456.41	0.25
−0.84	82.67	0.04	0.6	689.12	0.2	0.66	1459.68	0.25
4.35	84.15	0.04	0.6	690.45	0.2	0.15	1463.74	0.3
0.9	84.99	0.04	2.4	692.75	0.2	0.6	1465.65	0.25

UU IR Author Manuscript
UU IR Author Manuscript

Author's personal copy

University of Utah Institutional Repository
Author Manuscript

Table A1 (*continued*)

$Rp_i's$	$Er_i's$	$w_i's$	$Rp_i's$	$Er_i's$	$w_i's$	$Rp_i's$	$Er_i's$	$w_i's$
1.8	88.75	0.04	0.6	696.87	0.2	−0.15	1467.57	0.2
0.3	89.77	0.04	1.2	699.1	0.2	0.15	1469.52	0.2
−1.5	90.35	0.0068	0.6	702.55	0.2	0.15	1472.37	0.25
2.7	91.24	0.04	0.6	703.83	0.2	0.54	1479.7	0.25
0.6	92.54	0.0355	5.1	709.88	1	0.24	1483.01	0.25
−0.9	94.1	0.0055	0.6	715.75	0.2	0.45	1486.02	0.25
0.24	94.77	0.05	0.6	717.13	0.2	0.3	1494.8	0.25
0.3	95.6	0.04	0.6	718.9	0.2	0.24	1498.06	0.25
0.24	96.46	0.05	0.6	719.92	0.2	0.24	1500.95	0.25
1.2	98.1	0.022	0.6	721.59	0.2	0.45	1503.3	0.25
−0.9	101.54	0.0058	0.6	723.53	0.2	−0.3	1504.85	0.25
−0.9	101.7	0.009	0.6	727.41	0.2	0.45	1507.83	0.25
0.9	102.9	0.015	1.2	729.38	0.2	0.3	1511.82	0.25
0.72	105.19	0.015	9	733.36	0.15	0.24	1520.17	0.25
0.24	106.09	0.02	0.6	737.69	0.2	0.33	1524.9	0.25
−0.78	107.62	0.015	0.6	739.95	0.2	0.24	1527.7	0.25
−0.3	109.79	0.015	−1.05	741.74	0.45	0.24	1530.29	0.25
0.3	113.51	0.015	0.6	745.35	0.15	0.45	1533.32	0.25
0.6	115.92	0.015	0.6	747.06	0.15	0.15	1535.37	0.25
−0.39	117.59	0.015	0.6	750	0.35	0.24	1538.43	0.25
0.9	118.18	0.024	0.6	751.22	0.35	0.75	1541.51	0.25
0.45	118.8	0.03	0.6	754.05	0.1	0.15	1546.39	0.5
2.1	121.92	0.0138	3	758.84	0.25	0.6	1549.41	0.25
−0.15	122.92	0.05	0.6	761.71	0.25	0.24	1551.61	0.5
0.66	124.72	0.05	0.6	762.87	0.25	0.24	1553.94	0.4
−0.15	125.46	0.01	2.1	766.31	0.25	0.6	1559.77	0.25
1.5	126.02	0.025	0.15	767.99	0.25	2.79	1567.81	0.25
1.74	126.38	0.03	0.6	770.88	0.25	0.24	1570.94	0.4
0.48	128.1	0.03	0.6	772.63	0.25	0.6	1573.8	0.25
−0.3	130	0.03	1.2	778.46	0.1	0.24	1575.55	0.25
1.05	131.26	0.05	1.8	779.41	0.2	0.45	1579.2	0.25
0.84	132.16	0.05	0.6	782.38	0.2	0.66	1581.44	0.25
1.05	132.72	0.05	1.8	785.3	0.2	0.15	1587.27	0.5
1.35	133.54	0.05	0.6	790.32	0.2	1.26	1589.71	0.25
−1.2	134	0.1	0.6	792.61	0.2	1.35	1594.4	0.2
9	135.25	0.09	0.9	795.5	0.2	−0.39	1596.31	0.25
0.9	142	0.025	0.6	796.28	0.2	0.24	1598.54	0.25
1.5	145.53	0.0225	1.5	801.33	0.2	0.24	1600.54	1
0.3	147.29	0.0225	0.9	806.01	0.2	1.14	1604.4	0.25
0.6	149.06	0.018	1.2	806.95	0.4	−0.15	1606.4	0.25
0.3	149.93	0.025	0.6	810.11	0.4	0.15	1609.25	0.25
0.6	153.42	0.0125	0.6	812.76	0.3	0.15	1612.53	0.25
0.3	154.83	0.05	0.6	815.11	0.3	0.15	1616.18	0.25
0.3	156.75	0.02	0.6	817.9	0.3	0.15	1619.7	0.25
0.45	158.57	0.05	0.6	818.9	0.3	0.75	1622.2	0.25
0.45	159.08	0.05	0.45	821.86	0.3	1.35	1628.13	0.25
−0.33	160.94	0.009	0.45	823.55	0.3	−0.15	1630.18	0.25
1.95	163.6	0.04	0.45	825.51	0.3	0.66	1633.9	0.25
0.3	165.51	0.04	0.45	828.5	0.3	0.03	1637.74	0.25
0.75	166.27	0.04	0.45	830.13	0.3	0.3	1639.98	0.25
1.35	168.02	0.04	0.6	837.15	0.15	0.78	1644.06	0.25
0.36	169.33	0.04	0.6	843.03	0.15	1.2	1647	0.25
0.75	174.09	0.04	2.4	847.2	0.3	0.21	1650	0.25
1.14	174.52	0.04	0.3	851.29	0.3	0.03	1652.5	0.25
0.72	176.54	0.04	−0.3	852.33	0.3	1.23	1655.64	0.25
3	177.54	0.0175	0.3	854.9	0.3	1.2	1663.81	0.25
−0.3	178.45	0.0275	0.3	858.3	0.3	1.2	1665.9	0.25
−0.3	179.5	0.0325	1.5	861.36	0.2	0.33	1671.24	0.25
0.9	180.31	0.025	1.2	862.68	0.2	0.6	1672.77	0.25
0.3	181.99	0.025	0.6	866.17	0.3	0.45	1675.12	0.25
−0.9	188.54	0.015	1.5	867.95	0.2	0.75	1679.47	0.25
0.3	189.53	0.015	0.9	875.45	0.3	0.66	1681.55	0.25
1.5	192.32	0.022	0.6	879.06	0.3	1.2	1683.76	0.2
0.75	194.18	0.0375	0.6	881	0.3	−0.3	1685.43	0.25
3	198.55	0.1	0.6	883.81	0.075	1.05	1690.01	0.25
2.4	200.28	0.019	0.6	884.94	0.3	−0.15	1695	0.25
0.45	203.71	0.02	0.15	886.84	0.3	3.3	1699.63	0.25
0.6	207.02	0.02	0.3	892.69	0.3	0.21	1701.95	0.25
−0.39	207.58	0.02	−0.15	803.71	0.4	0.24	1702.96	0.25
−0.69	209.6	0.01	1.65	897.16	0.145	0.03	1706.86	0.25
0.3	210.72	0.05	0.6	898.5	0.25	0.09	1709.31	0.25
0.3	211.47	0.05	0.6	899.73	0.145	0.24	1713.64	0.25
1.29	213.65	0.02	0.3	901	0.25	0.3	1717.47	0.25
0.3	217.11	0.025	0.6	903	0.25	0.15	1720.12	0.25
3.9	220.62	0.06	0.6	906.09	0.145	0.45	1722.5	0.25

(*continued on next page*)

UU IR Author Manuscript
UU IR Author Manuscript

Author's personal copy

University of Utah Institutional Repository
Author Manuscript

Table A1 (*continued*)

$Rp_i's$	$Er_i's$	$w_i's$	$Rp_i's$	$Er_i's$	$w_i's$	$Rp_i's$	$Er_i's$	$w_i's$
2.4	221.76	0.09	0.3	908.82	0.2	1.2	1726.36	0.25
0.6	223.2	0.025	0.3	910.46	0.2	0.9	1731.66	0.25
−0.3	226.36	0.025	0.3	914.25	0.2	0.66	1735.01	0.25
0.45	226.82	0.03	0.6	916.1	0.1	0.15	1738.22	0.25
0.45	229.12	0.06	0.15	920.34	0.3	0.6	1741.22	0.25
3	231.45	0.048	0.9	923.05	0.1	0.75	1745.56	0.25
1.5	232.95	0.048	0.6	924.42	0.1	1.2	1749.6	0.22
1.2	233.94	0.075	0.3	926.53	0.2	0.3	1751.58	0.25
−0.3	237.09	0.04	0.45	929.56	0.1	0.15	1755.03	0.25
6	239.39	0.75	0.3	931.84	0.1	1.11	1760.23	0.25
1.47	241.16	0.025	0.3	934.66	0.1	0.6	1762.1	0.35
0.3	245.48	0.03	−0.6	940.09	0.3	1.2	1771.82	0.25
0.3	246.36	0.03	1.95	941.91	0.2	0.6	1774.44	0.25
0.3	247.87	0.03	0.18	944.72	0.2	0.9	1777.28	0.25
0.6	248.94	0.03	1.2	947.39	0.2	0.9	1779.3	0.25
0.3	251.56	0.06	0.15	949.25	0.2	0.75	1783.3	0.25
1.2	252.94	0.06	0.9	951.6	0.25	0.84	1788.37	0.25
1.35	253.65	0.06	1.2	953	0.85	0.15	1791.43	0.25
1.35	255.95	0.052	1.2	957.19	0.2	1.5	1794.88	0.18
9.9	261.65	0.052	0.3	959.78	0.2	0.15	1799.53	0.35
1.5	266.35	0.052	−0.75	961.17	0.2	0.6	1803.07	0.25
0.9	268.24	0.095	0.24	965.36	0.2	0.15	1808.12	0.6
3	270.01	0.095	0.24	967.88	0.2	0.75	1815.7	0.25
1.2	270.88	0.1	0.51	974.9	0.2	0.39	1819.56	0.25
2.4	272.78	0.07	1.14	978.14	0.2	1.44	1821.9	0.2
2.4	276.78	0.03	0.45	980.58	0.2	0.45	1825.24	0.25
1.8	279.84	0.065	0.6	983.69	0.2	0.3	1829.04	0.6
0.6	287.47	0.1	0.6	984.99	0.2	0.3	1830.74	0.6
3	289.46	0.1	0.3	986.79	0.2	0.9	1835	0.25
1.2	298.56	0.1	0.6	990.9	0.2	−0.3	1837.8	0.25
0.6	302.79	0.15	0.3	993.05	0.2	0.9	1839.86	0.22
0.6	305.12	0.1	0.3	998.23	0.2	0.3	1843.17	0.6
0.6	307.81	0.3	1.5	1001.05	0.2	2.1	1849.52	0.25
−0.6	308.99	0.1	0.3	1004.5	0.225	1.8	1857.55	0.2
0.6	312.48	0.3	−0.3	1005.67	0.2	0.15	1860.42	0.8
0.15	313.55	0.1	0.6	1007.5	0.2	0.36	1863.3	0.25
1.8	315.3	0.1	0.09	1010.49	0.2	0.3	1865.9	0.25
0.6	319.69	0.1	−0.24	1011.24	0.2	0.15	1868.3	0.25
1.5	323.46	0.1	−0.45	1014.7	0.2	1.02	1871.36	0.175
1.5	324.31	0.06	0.24	1015.91	0.25	0.3	1875.05	0.25
1.8	325.97	0.165	−0.3	1017.62	0.25	0.24	1877.8	0.25
−0.3	327.25	0.06	0.15	1019.08	0.25	0.6	1881.95	0.25
0.3	329.07	0.06	−0.3	1020.1	0.25	0.75	1885.1	0.25
0.3	330.53	0.075	0.15	1022.77	0.25	0.84	1889.61	0.25
0.45	332.51	0.06	0.54	1025.15	0.2	0.03	1893.33	0.25
1.5	334.05	0.1	0.3	1030.53	0.2	0.42	1897.04	0.25
0.75	336.61	0.06	1.2	1033.27	0.2	0.6	1902.6	0.25
3.45	340.07	0.06	0.15	1036.5	0.2	0.54	1906.65	0.35
0.15	342.32	0.075	0.9	1043.75	0.3	0.3	1910.42	0.35
1.14	343.95	0.06	0.75	1044.82	0.15	2.1	1915.5	0.3
1.11	346.98	0.06	0.6	1049.66	0.25	0.6	1902.6	0.25
−0.3	348.33	0.06	0.9	1053.64	0.25	0.54	1906.65	0.35
0.24	349.37	0.1	0.9	1056.08	0.25	0.3	1910.42	0.35
0.24	350.63	0.1	0.15	1059.8	0.25	2.1	1915.5	0.3
0.3	351.54	0.06	−0.42	1061.87	0.2	2.1	1917.54	0.3
0.3	353.02	0.06	0.6	1064.03	0.3	0.9	1922.7	0.3
0.54	355.33	0.06	1.8	1068.19	0.3	0.45	1924.5	0.3
−0.24	356.06	0.06	0.15	1071.4	0.3	0.6	1930.37	0.3
0.3	356.67	0.1	0.15	1074.62	0.3	0.9	1933.32	0.3
0.3	359.59	0.1	1.8	1076.83	0.225	0.9	1937.95	0.3
0.3	360.43	0.1	1.8	1077.74	0.2	1.5	1940.64	0.18
0.54	361.6	0.06	0.3	1080.06	0.2	0.9	1945.2	0.55
0.3	364.31	0.1	0.75	1082.56	0.3	0.6	1952.2	0.55
0.54	365.28	0.06	1.8	1084.2	0.25	0.75	1955.3	0.3
0.3	370.45	0.1	0.15	1086.75	0.25	0.9	1960.3	0.3
0.3	371.37	0.08	0.6	1089.92	0.4	0.66	1963.67	0.3
−0.3	372.6	0.06	1.2	1093.28	0.25	3	1967.8	0.18
0.3	373.32	0.075	0.3	1095.59	0.225	0.45	1972.71	0.5
0.3	377.78	0.075	0.6	1097.5	0.3	1.65	1977.16	0.15
1.8	379.81	0.075	1.65	1100.16	0.3	0.9	1979.7	0.3
0.75	383.32	0.075	1.5	1103.44	0.35	0.3	1983.8	0.75
1.05	387.47	0.0575	0.24	1108.42	0.35	0.3	1985.8	0.75
0.9	392.17	0.0575	−0.12	1110	0.2	0.9	1989.29	0.3
0.75	396.58	0.0575	0.21	1111.2	0.3	1.05	1993.6	0.22
0.3	402.3	0.1	−0.39	1113.7	0.3	0.3	1997.85	0.75

UU IR Author Manuscript
UU IR Author Manuscript

Author's personal copy

University of Utah Institutional Repository
Author Manuscript

Table A1 (*continued*)

$Rp_i's$	$Er_i's$	$w_i's$	$Rp_i's$	$Er_i's$	$w_i's$	$Rp_i's$	$Er_i's$	$w_i's$
0.75	405	0.1	0.3	1116.08	0.3	0.54	1999.84	0.75
0.6	408.45	0.1	0.6	1118.3	0.3	0.6	2002.45	0.3
−0.15	409.79	0.0575	0.6	1123.6	0.5	0.24	2006.36	0.3
0.3	410.63	0.2	0.3	1125.22	0.5	0.3	2008.22	0.3
0.3	414.18	0.2	0.3	1116.08	0.3	0.09	2010.9	0.3
0.9	415.61	0.2	0.6	1118.3	0.3	−0.15	2037.9	0.3
0.75	418.26	0.035	0.6	1123.6	0.5	0.15	2042.43	0.75
0.45	419.83	0.0575	0.3	1125.22	0.5	−0.36	2045.17	0.3
0.75	423.25	0.0575	0.3	1126.11	0.5	0.9	2050.17	0.3
0.84	425.46	0.09	0.75	1128.2	0.3	1.05	2053.18	0.3
0.3	427.54	0.08	2.1	1132.3	0.175	0.6	2054.84	0.3
0.3	428.76	0.07	0.15	1134.39	0.3	0.3	2058.85	0.75
0.75	430.53	0.09	0.3	1136.48	0.2	0.36	2063.75	0.3
1.5	433.81	0.0575	1.95	1139.08	0.3	0.36	2067.31	0.3
0.75	434.88	0.08	0.9	1143.43	0.115	0.3	2069.75	0.3
0.75	439.11	0.1	1.14	1146.66	0.115	0.54	2072.1	0.3
1.8	440.4	0.08	0.15	1149.9	0.3	0.15	2081.23	0.75
1.2	442.19	0.068	0.15	1152.79	0.3	0.75	2085.12	0.3
1.5	449.89	0.2	0.6	1156.1	1	0.54	2090.43	0.3
0.6	453.7	0.075	1.2	1159.65	0.1	1.26	2093.07	0.3
0.45	458.79	0.08	1.5	1161.5	0.2	0.6	2095.29	0.5
0.3	459.57	0.08	3.81	1163.3	0.3	0.6	2099.65	1
0.9	462.02	0.068	1.8	1165.23	0.2	−0.24	2106.22	1
2.55	463.8	0.068	3	1167.55	0.7	0.15	2108.78	0.3
0.75	2207.17	0.7	0.6	1170.27	0.1	0.15	2118.2	0.5
12	2213.88	2	1.5	1172	0.2	0.3	2121.42	0.3
10.95	2216.99	1	0.6	1174	0.3	0.15	2124.65	0.3
3.45	2223.71	0.45	0.6	1175.99	0.25	0.6	2129.05	0.4
3.45	2226.61	0.45	0.15	1178.6	0.3	1.8	2134.61	0.4
0.9	2233.24	0.45	0.3	1180.7	0.3	0.15	2137.75	0.3
0.9	2236.21	0.75	0.9	1184.41	0.3	−0.24	2141.9	0.75
3.6	2240.52	0.9	0.9	1187.46	0.3	1.95	2145.14	0.5
1.5	2247.9	0.35	0.3	1190.1	0.3	0.6	2148.5	0.3
0.6	2250	0.1	0.6	1192.67	0.3	0.6	2153.21	0.4
0.45	458.79	0.08	0.3	1194.18	0.3	0.3	2160.8	0.3
0.3	459.57	0.08	0.9	1198	1	0.6	2164.15	0.35
0.9	462.02	0.068	1.8	1200.8	0.15	0.6	2168.27	0.35
2.55	463.8	0.068	0.3	1204.56	0.3	−0.3	2172.9	0.75
0.3	466.61	0.1	−0.3	1206.15	0.125	1.8	2179.37	0.75
0.9	469	0.2	0.3	1207.49	0.25	2.25	2183.35	0.75
1.17	471.77	0.068	3.6	1214.2	0.5	0.9	2189.31	0.3
−0.24	476.6	0.068	0.3	1216.1	0.25	0.3	2199.99	0.4
0.6	477.25	0.2	0.54	1220.19	0.25	0.51	2202.8	0.3
1.56	479.28	0.068	0.66	1224.59	0.25	0.15	2207.17	0.3
1.65	481.33	0.068	0.3	1225.88	0.25	1.2	2213.88	0.6
0.3	483.56	0.09	0.75	1229.7	0.25	1.8	2216.99	0.6
0.3	485.29	0.09	0.3	1232.86	0.3	0.66	2223.71	0.3
0.3	487.1	0.09	0.3	1235.6	0.3	0.66	2226.61	0.3
0.6	489.55	0.09	0.3	1237.34	0.3	0.24	2233.24	0.3
0.75	490.47	0.068	0.6	1239.65	0.25	0.12	2236.21	0.3
0.66	495.7	0.087	0.6	1243.2	0.3	1.2	2240.52	1
1.5	500.28	0.1	1.2	1248.2	0.8	0.45	2247.9	0.4
0.9	502.01	0.1	0.3	1251.71	0.25	0.18	2250	0.1
0.9	503.36	0.1						

curves in Figs. 6–10: in blue[1] the MCNP moment, in red the Attila moment and in green the analytic moment. The experimental GODIVA moments are not plotted along with the other moments because values for the moments were only measured in two places; at the center of the sphere and at the sphere edge, 8.7407 cm. Table 4 is a summary of the moments calculated for the GODIVA experiment based on foil activation data from the McElroy report. The data and details of the McElroy report are not duplicated here and can be found in literature (see McElroy citation in the Bibliography of this paper).

[1] For interpretation of color in Figs. 1–11, the reader is referred to the web version of this article.

5. Results and discussion

Tables 4 and 5 show the results of validating moments from the three computational methods with the GODIVA experiment. Overall the NEDNDM compare very will well with the two computational platforms; Monte Carlo and the 30-energy group, S_N order, P_N order, finite element code Attila.

The most interesting comparison is the excellent agreement of the NEDNDM with the GODIVA experiment moments. The moments for GODIVA were calculated with the flux values in the energy bins found in the McElroy report. Table 4 shows the moments calculated at the GODIVA core center from the foil activation measurements. Table 5 is the T-O-F measurement for the 1st moment (mean energy) of the leakage neutrons from the surface of the

UU IR Author Manuscript
UU IR Author Manuscript

Author's personal copy

University of Utah Institutional Repository
Author Manuscript

Table A2
List of the $Rp'_m s$, $Er'_m s$ and $w'_m s$.

$Rp'_m s$	$Er'_m s$	$w'_m s$	$Rp'_m s$	$Er'_m s$	$w'_m s$	$Rp'_m s$	$Er'_m s$	$w'_m s$
3.00E−06	2350	5.00E+02	3.00E−06	7100	6.00E+03	7.50E−06	20500	1.60E+05
3.00E−06	2447	5.00E+02	3.00E−06	7200	7.00E+03	7.50E−06	21000	1.60E+05
7.50E−07	2548	1.00E+02	3.00E−06	7350	7.00E+03	1.50E−05	22100	1.20E+05
7.50E−07	2598	1.00E+02	3.00E−06	7500	7.00E+03	7.50E−06	23200	2.60E+05
7.50E−07	2672	2.00E+02	3.00E−06	7750	7.00E+03	1.20E−05	23700	2.60E+05
7.50E−07	2718	2.00E+02	3.00E−06	8000	7.00E+03	6.00E−06	24000	2.60E+05
6.75E−06	2800	2.50E+03	3.00E−06	8200	7.00E+03	1.20E−05	24200	2.60E+05
1.05E−06	2883	2.00E+02	1.50E−06	8400	7.00E+03	1.20E−05	24600	3.50E+05
2.25E−06	2960	1.00E+03	3.00E−06	8500	7.00E+03	1.20E−05	25000	3.50E+05
2.25E−06	3050	1.00E+03	3.00E−06	8750	6.00E+03	1.05E−05	25700	3.00E+05
2.25E−06	3150	1.00E+03	1.50E−06	9000	8.00E+03	1.05E−05	26200	3.00E+05
2.25E−06	3260	1.00E+03	3.45E−06	9150	8.50E+03	1.05E−05	27200	3.00E+05
2.25E−06	3356	1.00E+03	3.00E−06	9300	8.50E+03	1.05E−05	27500	3.00E+05
3.75E−06	3458	1.00E+03	3.00E−06	9500	8.50E+03	1.05E−05	28300	3.00E+05
3.75E−07	3574	1.50E+02	3.00E−06	9800	7.00E+03	1.05E−05	28800	3.00E+05
3.84E−07	3630	1.50E+02	1.20E−06	10000	6.00E+03	1.05E−05	29300	3.00E+05
3.00E−06	3700	1.50E+03	1.05E−05	10400	7.00E+04	1.05E−05	30000	3.00E+06
3.00E−06	3785	1.15E+03	1.05E−05	10650	7.00E+04	1.05E−05	31100	3.00E+06
1.50E−06	3858	8.00E+02	9.00E−06	10850	7.00E+04	9.90E−06	31800	3.00E+06
3.00E−06	3950	3.00E+03	1.35E−05	11200	7.00E+04	9.90E−06	32100	3.00E+06
9.00E−06	4050	7.50E+03	1.20E−05	11650	7.00E+04	9.90E−06	32800	3.00E+05
3.00E−06	4150	3.50E+03	7.50E−06	12000	7.00E+04	9.90E−06	34200	3.00E+05
3.60E−06	4250	3.50E+03	7.50E−06	12400	7.00E+04	9.90E−06	35000	3.00E+05
4.80E−06	4350	3.50E+03	9.00E−06	12800	7.00E+04	9.90E−06	36200	3.00E+05
6.75E−06	4500	3.50E+03	3.00E−06	12900	7.00E+04	9.90E−06	37000	3.00E+05
5.25E−06	4750	3.50E+03	9.00E−06	13100	8.00E+04	9.90E−06	37900	3.00E+05
3.75E−06	5000	3.50E+03	7.50E−06	13250	7.00E+04	9.90E−06	39100	3.00E+05
3.75E−06	5150	4.00E+03	7.50E−06	13700	7.00E+04	1.20E−05	40000	3.00E+06
3.75E−06	5350	5.00E+03	7.50E−06	14300	7.00E+04	1.20E−05	41000	8.00E+05
3.75E−06	5500	5.00E+03	7.50E−06	14800	7.00E+04	1.20E−05	42000	8.00E+05
3.75E−06	5600	5.00E+03	7.50E−06	15000	7.00E+04	0.0112	50000	9.00E+08
3.75E−06	5700	5.00E+03	9.00E−06	15300	7.00E+04	0.045	100000	1.80E+10
3.75E−06	5800	5.00E+03	9.00E−06	16000	7.00E+04	0.01	200000	7.50E+10
3.75E−06	6000	5.00E+03	1.20E−05	17200	7.50E+04	0.01	300000	8.00E+10
3.30E−06	6150	6.00E+03	9.00E−06	17900	7.00E+04	0.025	400000	5.50E+11
3.30E−06	6300	6.00E+03	9.00E−06	18400	7.00E+04	0.01	500000	1.00E+12
3.00E−06	6450	6.00E+03	7.50E−06	18900	7.00E+04	0.01	600000	1.00E+12
3.00E−06	6600	6.00E+03	7.50E−06	19400	7.00E+04	0.01	700000	9.00E+11
3.00E−06	6750	5.00E+03	7.50E−06	19800	1.60E+05	0.2	800000	2.40E+12
3.00E−06	6950	5.00E+03	7.50E−06	20000	1.60E+05	0.39	900000	4.00E+12

GODIVA experiment. The error in the tables is the relative error with the experimental value considered as the basis i.e.

$$\text{relative error} = \frac{|\text{experimental value} - \text{computational value}|}{\text{experimental value}} \times 100\%$$

The 1st moment, m_1 for GODIVA measured by the time of flight method (T-O-F) at the surface of the sphere is 1.55 MeV ± 2.9% (McElroy et al., 1969).Table 5 shows the comparison of the three computational methods to the T-O-F measurement. The * in Table 5 is the error associated with the experiment from the McElroy report and the ** is the error relative to the T-O-F measurement.

The plots in Figs. 7–11 below show the comparison of the moments from the three computational methods (MCNP5, Attila and NEDNDM). Moments were generated from MCNP5 by creating concentric spheres 1 cm radii away from each other, so for the MCNP model, nine spheres were modeled so a tally could be made at 1 cm increments up to the edge of the sphere (8.7407 cm). The MCNP5 tallies are f2 tallies over each surface and each tally was broken into 1000 evenly spaced energy bins up to 10 MeV. Energy bins from 10 MeV to 20 MeV showed large relative errors >20% and were omitted due to limits in computer power the authors have access to for this work (i.e. a 64-bit laptop with a hex core processor and 6 gigabytes of RAM). To get relative errors below 5% for energy bins from 1E−11 to 10 MeV the number of particles tracked in the MCNP model was 6million. The f2 tally data in each energy bin was then put in an excel spreadsheet and the various moments were computed numerically based on the definitions already presented for the mean, variance, skewness, kurtosis and higher order moments. Computing times for the MCNP5 calculations were roughly a day, 26.3 h, and Attila computation times were 3–4 h for a normal mesh of 0.01 cm which gave about 100,000 mesh nodes. The reason for the day time frame for MCNP was due to the high number of energy bins and particle histories needed to get in the 5% error range for the 1000 bins in the MCNP case Lab (2008).

Attila moments are created from the 30 group cross section file radion5 created by Transpire Inc. (energy bins are in Table 1). The data to create energy moments from Attila are from a custom report created in Attila where a line edit was made to collect the flux in each energy group at approximately 1 cm increments up to the system edge to match the MCNP5 sphere surface tallies. The points

Table A3
List of the $Rp'_n s$, $Er'_n s$ and $w'_n s$.

$Rp'_n s$	$Er'_n s$	$w'_n s$
1.52E+12	1.00E+06	1.00E+20
1.00E+10	2.00E+06	6.00E+16
3.80E+10	3.00E+06	8.00E+16
3.00E+09	4.00E+06	1.00E+16
5.10E+10	5.15E+06	8.00E+16
6.00E+10	7.00E+06	6.10E+16
1.50E+10	8.40E+06	1.50E+16
9.00E+09	9.40E+06	1.50E+16
1.20E+09	9.70E+06	3.00E+15

UU IR Author Manuscript
UU IR Author Manuscript

Author's personal copy

University of Utah Institutional Repository
Author Manuscript

along the line edit from Attila are not exactly 1 cm apart but close enough because each point lined up on a mesh point. The flux data in each energy group are numerically calculated similar to the MCNP5 method where the data was put in an excel spreadsheet and integrated according to the definitions already presented for the mean, variance, skewness, kurtosis and higher order moments. The reason why the Attila moments are higher than the GODIVA moments or the analytic and MCNP moments are because they are tuned to the fission spectrum which should give an expected mean energy value of about 1.98 MeV (Lamarsh and Baratta, 2001, p. 87) for a sphere like GODIVA. The higher order moments should be higher valued than GODIVA because of the fission spectrum weighting. Researchers (Sevast'yanov et al., 2000) claim that the fission spectrum for ^{235}U could be a superposition of 5 exponential functions and these researchers calculated an average energy value of 1.475 MeV ± 3.77%. Method of neutron energy moments is still diffusion based which is not perfect but the comparison plots show a good agreement with the transport codes general shape and the GODIVA experiment, meaning the faster neutrons populate the edges of the system or leak out because of the longer diffusion length or streaming effect of these fast neutrons.

The interesting thing about the NEDNDM is that they start to peel away from the MCNP moments right around 3 mean free paths from the boundary of the sphere, which is about 5 cm (if 1.1 cm is taken to be the average mean free path) and then correct back to the boundary value, due to the transport correction factor, r_0. Diffusion theory is valid in finite media at points that are more than a few mean free paths near the edge of the medium (Lamarsh, 1966, p. 129). The limitation of diffusion theory near the boundary of a source is noted and is not valid near the boundary which is why it is transport corrected (Glasstone and Sesonke, 1967, p. 112). Even though diffusion theory has its limits the results agree very well with GODIVA and MCNP. For multiphysics-engineering type calculations having a continuous energy solution quickly only 24% off in the highest moment (close to engineering limits i.e. 20%) is an excellent benefit that can be very useful to see multiphysics effects on nuclear reactors.

The shape of the functions for MCNP and Attila are very similar, the Attila moment functions have a sharper up turn and less of a parabolic shape which the NEDNDM and MCNP moments have. The reason for this could be the group structure of the radion5 neutron cross section file. The authors do not have control over this file and are thankful for the use of the code from Transpire Inc.

The dominate functional shapes that form the constants, CE's for the moments are from the last two summation terms in $F(E)$, see Eq. (20). If the resonance region was not included it would not have changed the value of the NEDNDM much for this case, because the contribution from the resonance summation was much smaller than the transition and fast region summations in Eq. (20). This makes sense for a fast reactor such as GODIVA. More work still needs to be done to see how reliable the method is for a broader set of reactor types i.e. thermal reactors.

6. Conclusions

The analytic EDNDE moments (0–5) has been validated with GODIVA. The NEDNDM agrees quite well with the GODIVA moments both at the core center and at the surface of the sphere. NEDNDM, MCNP5 and Attila moments agree with the experiment GODIVA in terms of showing that the higher energy or faster neutrons populate the outer radius of the sphere where they leak out of the system. This is seen by the difference in the value of moment 1 for all three computational moments and GODIVA at the center and the edge of the sphere. The NEDNDM results fall within the relative error bars associated with GODIVA results for all moments (0–5) calculated. The analytical moment results are much more accurate than the 30 energy group Attila simulation because of the reasons stated in Section 5 of this paper.

Acknowledgements

The authors would like to thank Transpire INC for use of the Beta version of Attila-7.1 in this research and the tutoring and explanations on how to use their excellent code.

Appendix A. Table of Constants for $F(E)$

Appendix A is the list of constants for each functional piece in the summations that make up $F(E)$, Eq. (20). The constant $Rp_0 = 85, \text{units } \frac{1}{\text{eV}}$ is not in a table. The energies, $Er'_{l,m,n}s$ are listed in eV. The $Rp'_{l,m}s$ are listed in eV/cm^2. The $Rp'_n s$ are listed in eV^4/cm^2. The $w'_{l,m}s$ are listed in eV^2. The $w'_n s$ are listed in eV^3.

(see Tables A1–A3)

References

Casella, G., Berger, R.L., 2002. Statistical Inference, second ed. Wadsworth Group Duxbury, Pacific Grove, CA, USA.

Crawford, D.S., Ring, T.A., accepted for publication. Verification of analytic energy moments for the one-dimensional energy dependent neutron diffusion equation with MCNP5 and Attila-7.1.0. Annals of Nuclear Energy, http://dx.doi.org/10.1016/j.anucene.2012.06.022.

Duderstadt, J.J., Hamilton, L.J., 1976. Nuclear Reactor Analysis. John Wiley & Sons, Inc., United States.

Foster, A.R., Wright, R.L., 1977. Basic Nuclear Engineering, third ed. Allyn and Bacon, Boston.

Glasstone, S., Sesonke, A., 1967. Nuclear Reactor Engineering. D. Van Nostrand Company, New York.

INL NEA/NSC DOC(95)03, September 2010. International Handbook of Evaluated Criticality Safety Benchmarks. INL, NEA/NSC.

Institute, K.A., 2000. Table of Nuclides, October 1. <http://atom.kaeri.re.kr/> (retrieved 05.07.11).

Kenny, J.F., 1947. Mathematics of Statistics, second ed. D. Van Nostrand Company Inc, New York.

Lab, L.A., 2008. A General Monte Carlo N-Particle Transport Code-Version 5. Los Alamos National Lab LA-UR-08-8617, Los Alamos.

Lab, L.A., 2000. ENDF/B-VII Incident-Neutron Data, July 5. <http://t2.lanl.gov/data/neutron7.html> (retrieved 05.07.11).

Lamarsh, J.R., 1966. Introduction to Nuclear Reactor Theory. Addison-Wesley Publishing Company, Reading, Massachusetts, USA.

Lamarsh, J.R., Baratta, A.J., 2001. Introduction to Nuclear Engineering, third ed. Prentice Hall, Upper Saddle River, New Jersey USA.

Lewis, E., Miller, W.J., 1993. Computational Methods of Neutron Transport. American Nuclear Society, La Grange Park, IL USA.

Lockheed Martin/ Knolls Atomic Power Laboratory, 2002. Chart of the Nuclides and Isotopes, 16th ed. Lockheed Martin/Knolls Atomic Power Laboratory, New York.

McElroy, W., Armani, R., Tochilin, E., 1969. Fast-Reactor Neutron Spectra and Foil-Activation Cross Section. Pacific Northwest National Laboratory, Richland, WA.

Morry, S., Williams, M., 1972. Neutron flux perturbations due to absorbing foils. Journal of Applied Physics, 6–18.

Sevast'yanov, V., Koshelev, A., Maslov, G.N.(, 2000. Representation of the fission spectrum of ^{235}U, ^{239}Pu and ^{252}Cf and the reactor spectrum as a superposition of five inelastic scattering functions. Atomic Energy, 292–299.

Weinberg, A.M., Wigner, E.P., 1958. The Physical Theory of Neutron Chain Reactors. The University of Chicago Press, Chicago.

UU IR Author Manuscript

UU IR Author Manuscript